THE JOURNAL OF PHYSICAL CHEMISTRY C

Article

pubs.acs.org/JPCC

In Situ Vibrational Study of the Reductive Desorption of Alkanethiol Monolayers on Gold by Sum Frequency Generation Spectroscopy

Jack Deodato C. Jacob, T. Randall Lee,* and Steven Baldelli*

Department of Chemistry, University of Houston, Houston, Texas 77204−5003, United States

Supporting Information

ABSTRACT: In situ sum frequency generation vibrational spectroscopy (SFG) was used to monitor the reductive desorption of decanethiol (DT) and octadecanethiol (ODT) self-assembled monolayers (SAMs) grown on evaporated gold on silica. At negative potentials, the alkyl chains of both monolayers became disordered as monitored by the appearance of methylene symmetric stretching modes in the collected spectra. The increased tilting of the terminal methyl groups on the chains of the DT monolayer further support this observation. The disappearance of the methyl C−H stretching vibrational modes at the reductive potential suggests that DT molecules diffused away from the surface after reduction. ODT molecules, on the other hand, retained their two-dimensional structure near the gold surface, implied by the strong methyl vibrational modes at the reductive potential. After four reductive cycles, a large portion of the DT SAM was fully desorbed, while the ODT monolayer existed as a combination of physisorbed and chemisorbed molecules on the gold surface, held in place by the van der Waals interactions between the alkyl chains.

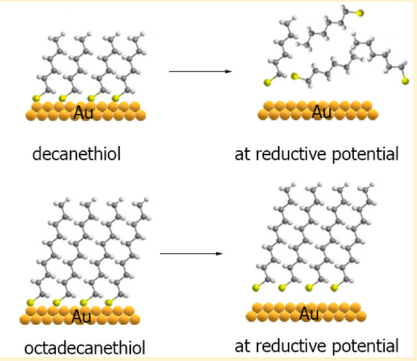

1. INTRODUCTION

Long-chain alkanethiols produce a well ordered and densely packed monolayer on metals,[1−3] which can act as a protective barrier against species (e.g., water, oxygen, and aggressive ions) that promote the corrosion process.[4−9] The process for producing these self-assembled monolayers (SAMs) is uncomplicated and can be done in a variety of solvents and under various conditions, due to their strong chemical affinity to metal surfaces. These characteristics have allowed these nanoscale films to be used in a variety of applications, such as lubricants for micromechanical systems[10] and sacrificial coatings for nanolithography.[11]

The electrochemistry of alkanethiolates on gold surfaces has been extensively studied.[12−20] Alkanethiols can be desorbed by the application of sufficient negative potential via a one-electron process:

$$RS - Au + e^- \rightleftarrows RS^-_{surface} + Au(0)$$

$$RS^-_{(surface)} \rightarrow RS^-_{(solution)}$$

After reduction, the thiolates can slowly diffuse away from the surface and dissolve into the bulk solution, depending on their solubility in that particular liquid. The electrochemical desorption of SAMs have found several potential uses in surface chemistry,[21] such as modifying the wettability of the surface,[22] producing phase-segregated binary SAMs, producing SAM microstructures,[23] controlled released of cells[19] or nanoparticles,[24] and recycling electrodes in biosensors.[25] Several studies have used the reductive desorption of SAMs to characterize the metal substrate[12] and monolayer coverage.[20] The reductive potential of alkanethiol SAMs in alkaline solutions was found to depend on several factors, such as the pH of the electrolyte solution, the nature of electrolytes, and the length of the alkyl chain. As the pH was decreased from 13.7 to 5.9, the reductive peak was observed to broaden and shift to the positive direction. It was found that using three different bases, the reductive peak required a greater overpotential in LiOH solutions relative to NaOH and KOH solutions.[12] Furthermore, the reductive peaks shifted to the negative direction as the chain length increased.[12]

The oxidative readsorption of these alkanethiol monolayers was also found to depend on the length of the alkyl chains.[12] Previous studies revealed that, depending on the solubility of the desorbed molecules, these thiolates either readsorb to the surface or diffuse into the solution.[13,26] Several authors have proposed various mechanisms for monolayer desorption. One theory is that once desorbed, alkanethiolates form bilayers[11] or micelles,[27,28] while another theory is that SAMs retain their two-dimensional monolayer structure.[29] These structures provide a means for the thiolates either to readsorb on the surface or to diffuse into the solution.

In situ infrared (IR) spectroscopy measurements of the reductive desorption and readsorption of SAMs on gold have found that these monolayers become more disordered after desorption.[14,30] Ex situ sum frequency generation (SFG) spectroscopic studies of alkanethiolate SAMs before and after desorption have found that SAMs formed from 10- and 12-

Special Issue: John C. Hemminger Festschrift

Received: May 6, 2014
Revised: September 26, 2014
Published: October 9, 2014

   dx.doi.org/10.1021/jp504463z | J. Phys. Chem. C 2014, 118, 29126−29134

carbon chain alkanethiols desorb after 30 CV scans, while those formed from 16- and 18-carbon chain alkanethiols retain their crystalline structure.[31] The goal of our study is to utilize SFG to monitor alkanethiol adsorbates as they desorb from a gold surface in situ in an effort to understand more completely the nature of the desorption process.

2. EXPERIMENTAL SECTION

2.1. Materials. Octadecanethiol (ODT; >98%, Sigma-Aldrich), decanethiol (DT; >98%, Sigma-Aldrich), potassium hydroxide (85%, Sigma-Aldrich), and ethanol (100%, Aaper) were used as received without further purification. Tetrahydrofuran (>99%, Sigma) was distilled to remove the butylated hydroxytoluene (BHT) stabilizer before use. Deuterium oxide (D, 99.9%) was purchase from Cambridge Isotopes Laboratories Inc.

2.2. Gold Film Preparation. Chromium (100 Å) and gold (1000 Å) were thermally evaporated onto silicon(100) wafers at a rate of 1 Å/s at a vacuum pressure of $\sim 10^{-6}$ Torr in a chamber equipped with a diffusion pump. After the deposition, the chamber was cooled to room temperature and flushed with ultrapure nitrogen gas. The gold-coated wafers were cut into slides (~1 cm × 3 cm) and rinsed with ethanol before use. Topography characterization of the gold samples was performed with an Agilent 5500 atomic force microscope using Sharp Nitride Lever (SNL) tips from Bruker. All scans were done in contact mode. Grain size was determined using the grain SPM software (Gwyddion).[32]

2.3. Preparation of SAMs. The gold slides were immersed in 1 mM thiol ethanolic solutions and allowed to equilibrate for 48 h. The resultant SAMs that formed on the gold surfaces were thoroughly rinsed with THF and ethanol, and then blown dry with ultrapure nitrogen gas before characterization using SFG spectroscopy.

2.4. Experimental Setup. SFG spectroscopy has been presented elsewhere,[33−35] and a detailed description of this technique is provided in the Supporting Information. Cyclic voltammograms were taken using a 263A Princeton Applied Research Potentiostat/Galvanostat with a PAR M5210 lock-in amplifier controlled by the PowerSuite software. A platinum wire was used as the counter electrode, and the reference electrode was Ag/AgCl in saturated KCl.[36] Cyclic voltammetric measurements were conducted from −0.3 to −1.35 V at a scan rate of 50 mV s^{-1}. The potential was initially swept toward the negative to reduce the SAM molecules and then reversed to reoxidize the reduced thiolates. The gold substrate was mounted at the bottom of an electrochemical cell using an O-ring and a clamp. The solution of the cell was deaerated by bubbling N_2 gas for 30 min before analysis, and the cell was placed under a nitrogen atmosphere during the electrochemical measurements. The area of the working electrode was determined by the area of the exposed surface, which in turn was equal to the area within the O-ring, 1.69 cm^2. Electrochemical impedance spectroscopy (EIS) measurements were performed in the same cell.

For the in situ monitoring of alkanethiol desorption by SFG spectroscopy, the SAM-coated gold slide was immersed in a deaerated 0.1 M NaOH−D_2O solution and then covered with a CaF_2 window (Figure 1). A custom-made Ag/AgCl in saturated KCl electrode was used as the reference electrode,[36] and a hydrogen flame-annealed platinum wire was used as the counter electrode. To complete the connection, a gold wire, flattened to a thickness of ~50 μm, was placed between the gold slide and the window. The cell was fully deaerated by bubbling with nitrogen gas for 30 min and was kept in an enclosure constantly being flushed with nitrogen gas. A 263A Princeton Applied Research potentiostat/galvanostat controlled the potential of the cell during operation.

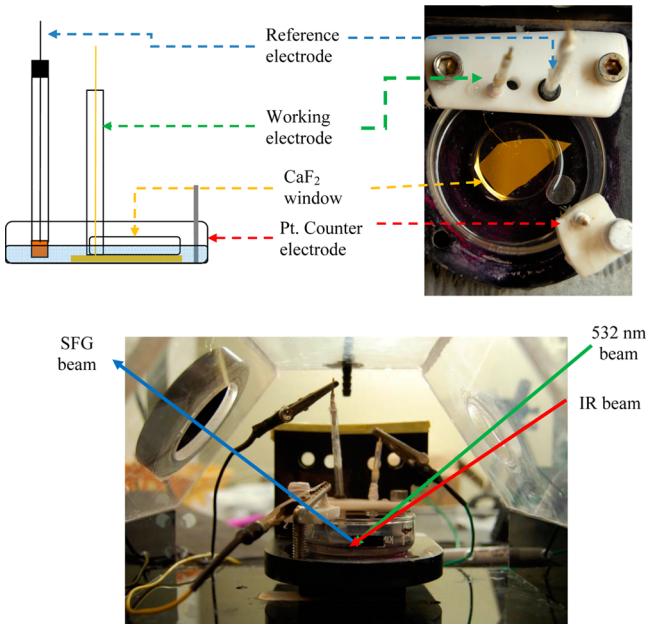

Figure 1. (Top) Illustration of an SFG electrochemical cell. (Bottom) The cell is placed in an enclosure filled with nitrogen gas.

3. RESULTS AND DISCUSSION

3.1. Electrochemistry. The cyclic voltammograms of DT and ODT monolayers on gold are shown in Figure 2. For DT SAMs, two broad current peaks are observed at the first cathodic sweep. The first peak at −1050 mV was assigned as the reductive peak, and the peak at −1250 mV was assumed to be from the desorption of thiols on the gold defect sites or from hydrogen evolution. These peaks are similar to those observed in previous studies.[27,31] The oxidation peak, which is attributed to the reoxidation of the thiolates on the gold surface,[27] is noticeably absent at the return sweep. The second cathodic sweep features a weaker reductive peak at −1050 mV, suggesting that only a fraction of the decanethiolates reoxidized on the surface. For the third cycle, the reductive peak is even weaker, suggesting that even more of the thiolates were not readsorbed onto the surface.

ODT SAMs, on the other hand, exhibited two reductive waves at −1100 and −1250 mV at the first cathodic sweep. The reductive potential of the ODT adsorbates occurs at a lower potential than for DT owing to either the decreased ion permeability of the monolayers due to the increased intermolecular interaction between the alkyl chains[13] or to a decrease in the fractional drop of the applied potential across the monolayer as the alkyl chain increases.[12] For the anodic sweep, a small broad peak is observed at 950 mV and is assumed to be caused by the reoxidation of the thiolates.[27] As observed for DT, the second cathodic sweep features weaker reductive peaks. The third and all subsequent cycles shows one reductive wave at −1100 mV, and a small oxidation peak at −950 mV, suggesting that the monolayer desorbs and partially readsorbs on the gold surface. The decreasing magnitude of the

dx.doi.org/10.1021/jp504463z | J. Phys. Chem. C 2014, 118, 29126−29134

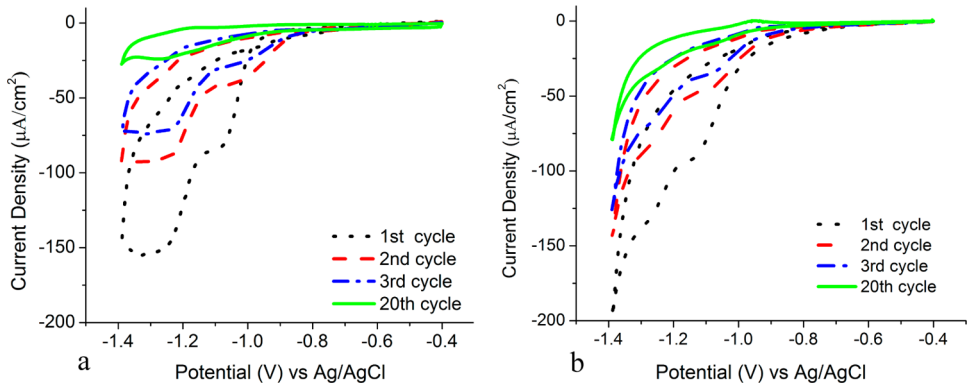

Figure 2. Cyclic voltammogram of (a) DT and (b) ODT monolayers on gold in 0.1 M KOH aqueous solution.

succeeding reductive peaks again suggests that not all of thiolate molecules undergo reoxidation.

3.2. Sum Frequency Generation. All SFG spectra in this study were taken with both input beams and the SFG output beam set to p-polarization or ppp. The assignment of the observed modes are the methyl symmetric C−H stretch (r^+) and its Fermi resonance (r^{FR}) at 2870 and 2935 cm^{-1}, respectively, and the methyl antisymmetric out of plane (rb^-) and in-plane (r^-) C−H stretching modes at 2955 and 2965 cm^{-1}, respectively. Also included in the fitting are the methylene symmetric C−H stretching (d^+, 2850 cm^{-1}) and its Fermi resonance stretching (d^{FR}, 2915 cm^{-1}) modes.

Long-chain alkanethiols such as DT and ODT form well-ordered monolayers with the alkyl chains aligning to an all-trans configuration, where there is a local inversion at the middle of each C−C bond. Thus, methylene stretching modes are not observed in crystalline monolayers and the presence of methylene stretching modes are qualitative indicators of kinks[34] and gauche defects, and the d^+/r^+ ratio is a useful indicator of conformational disorder.[37]

The ratio of the symmetric and antisymmetric methyl C−H stretch (r^+/r^-) can be used to estimate the average tilt of the terminal methyl group. Orientation analysis was done by deriving the intensity ratios of the symmetric and antisymmetric stretching modes of the terminal methyl groups from the curve fitting. These ratios were then compared to theoretical orientational curves, and the methyl group tilt was approximated using the bond polarizability model devised by Hirose[38,39] and Wang.[40] This approximation assumes that the monolayer surface is rotationally isotropic about the surface normal, and the local symmetry of the methyl group is near C_{3v}.

3.2.1. Reduction of the DT SAM. The SFG spectra of the DT chains on gold during the first reductive reduction cycle are shown in Figure 3. The spectrum acquired before reductive desorption, as shown in the topmost plot, reveals that the spectrum is dominated by peaks associated with the r^+ and r^- modes. At −400 mV, the r^+/r^- ratio of the DT SAM is consistent with a methyl group tilt angle of ∼37°, which is consistent with tilt angles associated with densely packed SAMs, derived from alkanethiols with an even number of carbons in the chain.[42] Methylene C−H stretching modes (d^+ and d^-) at 2850 and 2915 cm^{-1} are not evident, suggesting that the monolayer is well-ordered and crystalline.

At −800 mV, the peak for the methylene symmetric C−H stretching vibration (d^+) appears, suggesting that the monolayer is becoming more disordered at this potential. At −1050 mV, all resonant signals disappear, indicating that the monolayer has

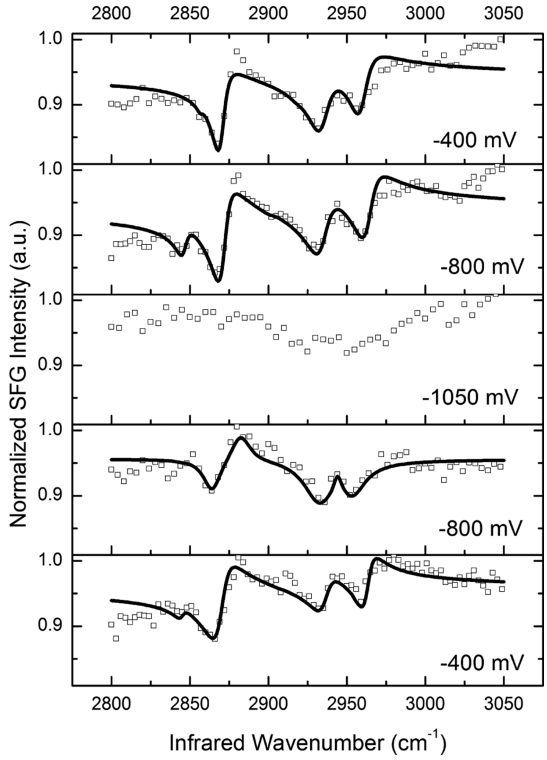

Figure 3. Normalized SFG spectra of a DT SAM on gold obtained during the first reductive desorption cycle, proceeding from the top down as labeled.

been desorbed. The current density at this potential is estimated from the CV analysis to be 68 $\mu A/cm^2$ (Table 1). Upon returning the potential to −800 mV, the peaks associated with the methyl C−H stretching vibrations start to reappear, but are weaker in intensity than the previous spectrum at −800 mV. When the potential was set back to −400 mV, more of the thiolate chains readsorb and reform the monolayer, as seen from the increase in the intensity of the band associated with r^+. However, the intensity of this band after the cycle is much lower than that of the initial monolayer, likely because the monolayer is no longer well packed, and the alkyl chains are more disordered. The presence of the methylene C−H stretching modes at 2850 and 2915 cm^{-1} verifies that the monolayer has more gauche defects due to this disordering. These results are in agreement with that of the CV experiment, that the DT SAM desorbs and a fraction of the monolayer reabsorbs to the surface.

dx.doi.org/10.1021/jp504463z | J. Phys. Chem. C 2014, 118, 29126−29134

Table 1. Methyl Group Tilt Angles and d^+/r^+ Values for a DT SAM at Various Potentials

	potential (mV)	methyl group tilt angle (deg)	d^+/r^+	current density (μA/cm^2)
	−400	37 ± 5	NA	0 ± 2
	−800	43 ± 5	0.3 ± 0.15	3 ± 2
1st cycle	−1050	NA	NA	68 ± 2
	−800	48 ± 5	NA	7 ± 2
	−400	42 ± 5	0.1 ± 0.09	0 ± 2
2nd cycle	−400	50 ± 5	NA	0 ± 2
3rd cycle	−400	49 ± 5	NA	0 ± 2
4th cycle	−400	69 ± 5	NA	0 ± 2

Table 2. Methyl Group Tilt Angles and d^+/r^+ Values for an ODT SAM at Various Potentials

	potential (mV)	methyl group tilt angle (deg)	d^+/r^+	current density (μA/cm^2)
	−400	29 ± 5	0.1 ± 0.08	0 ± 2
	−800	31 ± 5	0.2 ± 0.08	8 ± 2
	−1200	30 ± 5	0.3 ± 0.15	101 ± 3
1st cycle	−1350	29 ± 5	0.1 ± 0.09	156 ± 3
	−1200	30 ± 5	0.3 ± 0.15	46 ± 2
	−800	30 ± 5	0.2 ± 0.13	5 ± 2
	−400	32 ± 5	0.1 ± 0.08	0 ± 2
2nd cycle	−400	35 ± 5	0.1 ± 0.08	
3rd cycle	−400	35 ± 5	0.1 ± 0.08	
4th cycle	−400	36 ± 5	0.1 ± 0.08	

3.2.2. Reduction of the ODT SAM. Figure 4 shows the SFG spectra of ODT on gold during the first desorption cycle. At

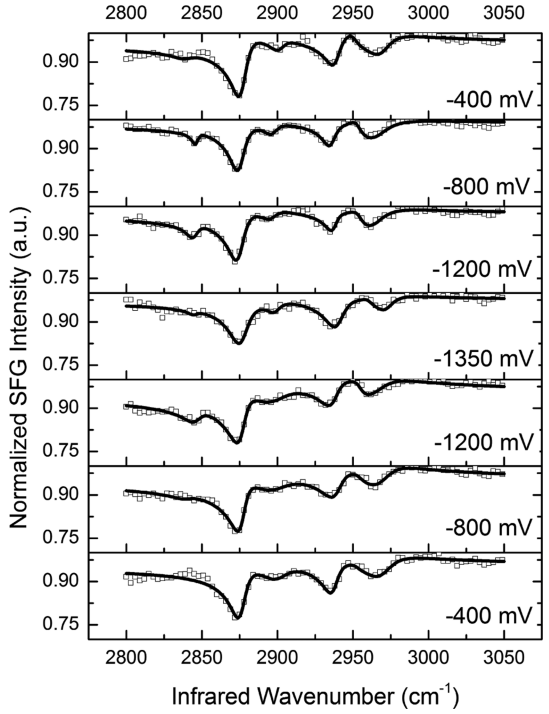

Figure 4. Normalized sum-frequency spectra of ODT on gold obtained during the first reductive desorption cycle, proceeding from the top down as labeled.

−400 mV, only the methyl C−H stretching modes are evident, with no methylene CH stretching resonances, indicating that the monolayer is well ordered. The initial methyl group tilt angle is calculated to be 29°. At potentials of −800 and −1200 mV, the methyl group tilt angle remained constant at ∼30°, but methylene C−H stretching resonances at 2850 and 2915 cm^{-1} appeared in the spectra, suggesting a disruption in the order of the alkyl chains during the reductive sweep. As thiolate monolayers are reduced and lift off the surface, the monolayer becomes less packed, allowing gauche defects to form.[34,41−44]

At −1350 mV, the methyl group tilt angle increases slightly to 29°. From the CV experiment in Figure 2, the current density at this potential is estimated to be 156 μA/cm^2 (see Table 2), which indicates that reduction is taking place at this potential. However, as observed from the SFG spectra in Figure 3, the ODT monolayer remains intact at this potential. At more negative potentials, bubbles began to form on the gold surface, probably due to hydrogen evolution.

It should also be noted that the intensity of the methylene C−H stretching mode decreased as the potential was decreased to −1200 mV to −1350 mV. The majority of gauche defects are believed to be localized at the alkyl chain near the gold surface.[41] The constrained Au−S−C bond prevents the all-trans configuration on nearby carbon bonds. As individual alkanthiolates slowly detach from the surface at −800 and −1200 mV, more gauche defects appear, but when the monolayer completely desorbs at −1350 mV, the alkyl chains are free to realign to the trans state, lowering the number of methylene groups visible to SFG. It is interesting to note that after setting the potential back to −800 mV, the methylene C−H stretching modes disappear, suggesting that the conformational disorder observed at negative potential is reversible.

3.2.3. Multiple Reduction Cycles. Additional reductive desorption cycles on the DT and ODT monolayers were performed, and the corresponding SFG data are shown in Tables 1 and 2. For clarity, only the first and fourth desorption cycles for each adsorbate are presented in Figure 5. For DT (Figure 5a), the top spectrum shows no discernible resonances, implying that, at the reductive potential (−1050 mV), the monolayer desorbs and diffuses away from the surface. As shown in Figure 3, however, a fraction of the thiolates can still readsorb. After four cycles, the intensities of the methyl resonances have drastically diminished, and the methyl tilt angle is estimated to be ∼70°. This large tilt suggests that the monolayer became disordered, with the alkanethiolates nearly flat on the surface in a low-density phase.[9] In contrast, the ODT monolayer still retained the original crystalline structure after four desorption cycles (Figure 5b).

3.3. Discussion. *3.3.1. Cyclic Voltammetry.* The CV scans of both DT and ODT show multiple reductive waves. For octadecanethiolates on SAMs, the first peak at −1100 mV is assumed to arise from thiolates on regions where gold has a (111) orientation.[42] The reductive peak at −1250 mV might come from the desorption of thiols on the steps and defect sites of the gold substrate, with some contribution from hydrogen evolution.[41−45]

dx.doi.org/10.1021/jp504463z | J. Phys. Chem. C 2014, 118, 29126−29134

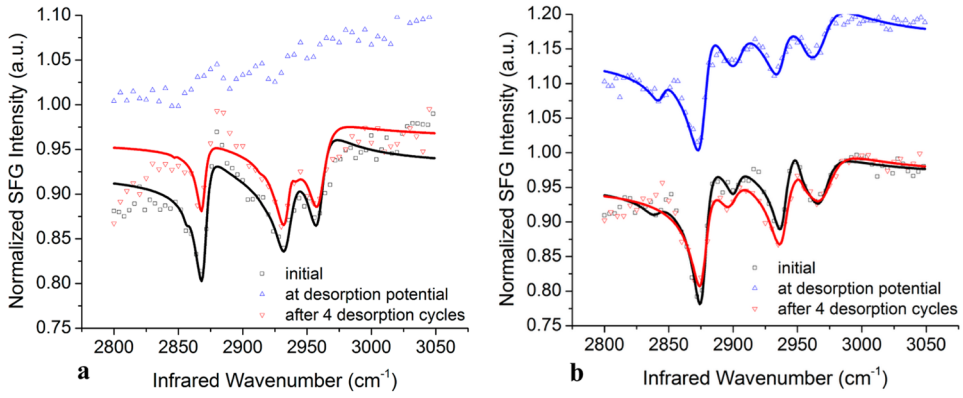

Figure 5. Normalized sum frequency spectra of (a) DT and (b) ODT monolayers on gold during four reductive desorption cycles. The spectra taken at desorption potential were offset by +0.1 for clarity.

The oxidative wave that signals reoxidation of the thiolates on the gold surface could not be detected in the CV scan of the DT monolayer and was weak for the ODT monolayer; these results contrast those from studies that utilized Au(111) single crystals as substrates, which gave strong reductive and oxidative peaks.[10,21,29] Au(111) single crystals typically have a rough mean square (rms) roughness of 1−4 Å.[43] The substrates for the present study are evaporated gold on silicon wafers, which are polycrystalline in nature and have an rms roughness of 15 Å. Previous electrochemical studies of SAMs on polycrystalline gold could only detect a weak double-layer charge, or multiple reductive peaks and a weak oxidative peak.[44−46] Thiolates desorb and readsorb on sites with different crystallographic orientations at different potentials,[47] which might cause the oxidative peak to broaden and weaken in intensity. The oxidative current could not be used to quantify the readsorption of the alkanethiols because, thiolate reduction overlaps the hydrogen evolution current on polycrystalline gold.[13,48]

3.3.2. Surface Coverage Estimation by Cyclic Voltammetry. Integrating the desorption peak at −1050 mV, the reductive charge of the DT SAM at the first sweep was estimated to be 140 $\mu C/cm^2$, far larger than those reported in other studies.[12,13,49] The ODT SAM shows a similar reductive charge of 170 $\mu C/cm^2$. These values are higher than the theoretical reductive charge of 70 $\mu C/cm^2$, which corresponds to the 7.2×10^{-10} mol/cm^2 coverage for a fully formed monolayer $(\sqrt{3} \times \sqrt{3})R30°$ on gold.[50] This difference might be due to surface roughness of the gold substrate,[51] which increases the actual surface area,[12] and the non-Faradaic contribution due to capacitive charging.[12,13,46,52] The overlap between the reductive peak and the hydrogen evolution also complicates the computation of the desorption charge.

Because reductive desorption is a one-electron process, the reductive charge can be used to estimate the surface coverage. Taking the ratios of the reductive charges can be used to estimate the extent the monolayer is reduced and oxidized at each cycle. At the second reductive sweep of the DT SAM, a value of 99 $\mu C/cm^2$ was obtained, suggesting that only 70% of the monolayer reoxidized on the gold surface (Table 3). After the second cycle, 61% of the thiolate reoxidized, as shown by the reductive peak at the third sweep. The reductive charges obtained from ODT SAM at different consecutive sweeps suggest that only 60% of the monolayer is reoxidized after every sweep. The incomplete reoxidation of both SAMs might be due to the thiols diffusing away from the surface into the bulk of the solution or the formation of disulfides.[31]

Table 3. Reductive Charge of DT and ODT SAMs on Gold at Consecutive Voltammetric Cycles

SAM molecule	cycle	reductive charge ($\mu C/cm^2$)	percent reoxidized previous cycle
DT	1st	140	
	2nd	99	70
	3rd	61	62
	4th	22	35
ODT	1st	170	
	2nd	105	62
	3rd	62	59
	4th	34	55

3.3.3. Conformational Disorder at Nonreductive Potentials. At potentials more positive than the reductive potential, methylene C−H stretching modes appear in the SFG spectra of both DT and ODT monolayers, suggesting the chains have become more disordered. It is possible that the observed methylene resonances are from gauche defects caused by the desorption of thiolates on defect sites such as those near the grain boundaries of the gold substrate.[42,53,54] Alkanethiol domains are more loosely packed on defect sites than on terraces and are more prone to desorption. Once detached from the gold surface, these domains become more loosely packed, and gauche defects arise. The fact that these methylene CH resonances disappear at more positive potentials support this hypothesis. At oxidative potentials, the thiolates reattach to the surface, reestablishing the all-trans configuration and eliminating gauche defects.

It has been observed in EIS measurements that alkanethiol monolayers produce defects and become more permeable to ions and water at reductive potentials more positive than the reductive potential.[55−58] The cause of these defects are still unknown, but it has been hypothesized that at negative potentials, the electric field exerts a torque on the headgroups, causing conformational disorder on alkyl chains located at the domain boundaries, which are less dense and have more conformational degrees of freedom than the chains at the center of the domain.[59]

3.3.4. Reduction of DT and ODT SAMs on Gold. SAMs formed from DT and ODT behave differently at their reductive potentials as observed from their SFG spectra. The methyl C−H stretching resonances disappear in the spectra of DT on gold at −1050 mV, suggesting that the thiolates have diffused away from the gold surface. SAMs derived from ODT, on the other

dx.doi.org/10.1021/jp504463z | J. Phys. Chem. C 2014, 118, 29126−29134

hand, still show strong methyl symmetric C−H modes, indicating that though desorbed, the monolayer is still conformationally intact and near the gold surface. This disparity can be attributed, at least in part, to the difference in the solubilities of the desorbed thiolates in the 0.1 N KOH solution. DT is slightly soluble in alkaline solutions (~1.2 mg/L or 6.9×10^{-6} mol/L),[29] while the solubility of ODT in water is less than 5×10^{-4} mg/L or 1.7×10^{-9} mol/L.[60] Estimating the space between the gold film and the CaF_2 window is 50 μm, the volume of liquid under the CaF_2 window (2.54 cm diameter) can be approximated as 2.2×10^{-5} L. At full coverage, the surface concentration of DT and ODT on gold is estimated to be 7.2×10^{-7} mol/cm^2. Once desorbed, the concentration of DT and ODT thiolates in the liquid would both be $\sim 1.7 \times 10^{-4}$ mol/L. Thus, a fraction of the decanethiolates can plausibly dissolve and diffuse away from the gold surface to the bulk of the solution and thus escape detection by SFG spectroscopy. This conclusion is supported by in situ fluorescent microscopy studies by Bizzoto and co-workers, which showed that thiols desorb as thiolates at negative potentials and diffuse away from the surface.[61] In addition, the stronger van der Waals interactions between the ODT chains, when compared to the shorter DT chains,[1] causes the ODT molecules to be locked into a crystalline formation as a physisorbed monolayer that can reoxidize to the surface.

4. SURFACE DENSITY VERSUS POTENTIAL

Since the peak amplitude is proportional to the number of molecules on the surface (eq 7 in Supporting Information), the amplitude of r^+ can be used to estimate the density of the monolayers at different potentials in the desorption process. As shown in Figure 6, the normalized r^+ amplitudes of DT SAMs dropped to zero at the reductive potentials. ODT monolayers, however, still retained a strong r^+ amplitude at reductive potentials, despite the large current running through the surface. It should also be noted that the r^+ amplitude of DT decreased at subsequent cycles, suggesting that a portion of the decanethiolates slowly diffused away from the surface during the reduction. The ODT monolayer, on the other hand, remained a densely packed film after four redox cycles.

5. NATURE OF DESORBED ALKANETHIOLATES

There is still much debate regarding the exact nature of a reductively desorbed monolayer. In addition to possibly forming bilayers or micelles, desorbed octadecanethiolates might also form disulfides or as thiolates.[31,60]

The EIS Bode phase plot shown in Figure 7 provides additional information on the nature of the ODT monolayer after desorption. An ex situ XPS study showed that ODT completely desorbs at potentials lower than −1200 mV.[49] Further, a previous EIS study observed that after ~30 reductive CV cycles, a DT monolayer on gold fully desorbed from the surface, while the corresponding ODT monolayer was intact.[31] We thus performed 10 CV sweeps on ODT SAM on gold in 0.1 M NaOH solution from −400 to −1350 mV. The SAM was analyzed by EIS from 100 kHz to 1 Hz before and after the CV experiment. Ideally, a well-ordered SAM should have a phase angle of 90° in a Bode phase plot at the low frequency range (1−1000 Hz) where diffusion dominates. After 10 cycles, the phase angle of the monolayer at the low frequency range dropped from 84 to 81°, suggesting the SAM retained its low ion permeability, which is in agreement with the previous

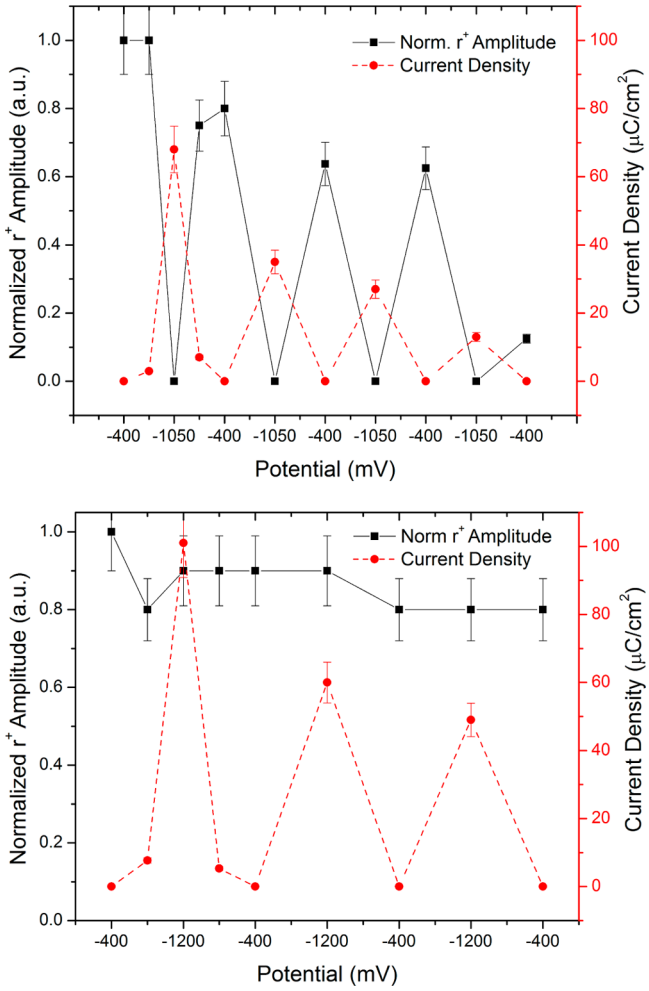

Figure 6. Normalized r^+ amplitudes and current densities of (top) DT and (bottom) ODT SAMs at different cathodic potentials.

study.[31] After a thorough washing of ethanol, the phase angle decreased to 66°, indicating that the resulting monolayer was composed of physisorbed molecules, plausibly held in place by the thiolates still chemisorbed to the surface. These thiolates are more soluble in ethanol than in water, and thus a portion was likely removed after the subsequent washing, decreasing the monolayer density and causing the monolayer to be more permeable. Figure 7b shows the SFG spectra of the monolayer before and after CV. Even after 10 CV cycles and a thorough washing with ethanol, the SFG spectrum was still consistent with that of a well-ordered monolayer. A method to characterize the desorbed molecules is needed to understand fully the nature of the desorbed monolayer.

Based on the results shown in Figure 4, we conclude that reduced octadecanethiolates do not form micelles or bilayers; this occurrence would lead to a rearrangement of the alkanethiolate chains, which would be detected in the SFG spectra as the disappearance of the methyl C−H stretching modes at reductive potentials. That SFG spectroscopy can still detect the methyl C−H stretching modes from ODT at desorption potentials suggests that, even though the monolayer has been fully reduced, its low solubility in water and the van der Waals interactions of its alkyl chains allow it to retain its crystalline structure. This interpretation is consistent with a model in which octadecanethiolates exist as a two-dimensional monolayer on the surface with little or no micelle formation.[31]

dx.doi.org/10.1021/jp504463z | J. Phys. Chem. C 2014, 118, 29126−29134

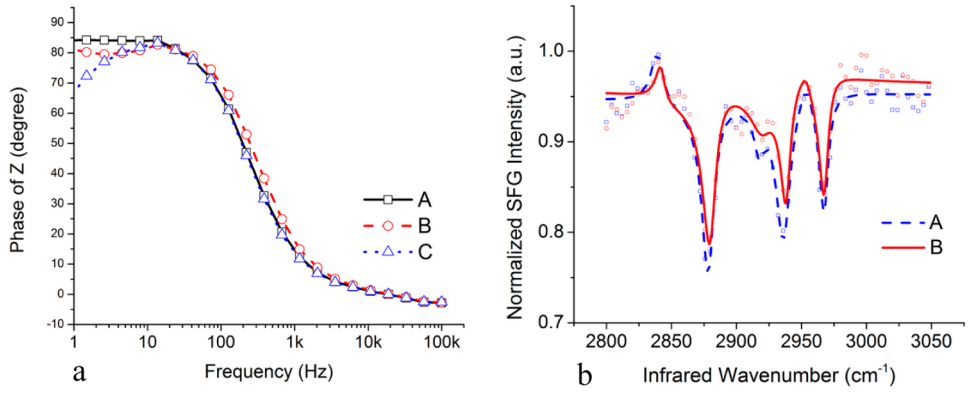

Figure 7. (Left) EIS Bode phase of an ODT SAM on gold (a) before and (b) after 10 CV cycles and (c) after washing with ethanol. (Right) SFG spectra of ODT on gold (A) before and (B) after 10 CV cycles and washing with ethanol.

6. CONCLUSIONS

Reductive desorption of DT and ODT SAMs grown on evaporated gold on silica were monitored using in situ sum frequency generation. Negative potentials caused disordering in the alkyl chains, as indicated by the appearance of d^+ modes in the collected spectra. At reductive potentials, DT thiolate molecules diffused away from the surface, while ODT thiolate molecules retained their two-dimensional structure near the gold interface. After four cycles, a large portion of the DT SAM was fully desorbed, as indicated by the methyl group tilt angle, while a majority of the ODT monolayer existed as a physisorbed layer on the gold surface, held in place by the interactions between the alkyl chains of molecules still chemisorbed to the surface.

■ ASSOCIATED CONTENT

Ⓢ Supporting Information

The full CV scans of the two monolayers are presented, along with the description of the SFG spectroscopy setup and curve fitting parameters. This material is available free of charge via the Internet at http://pubs.acs.org.

■ AUTHOR INFORMATION

Corresponding Authors

*E-mail: trlee@uh.edu.

*E-mail: sbaldelli@uh.edu.

Notes

The authors declare no competing financial interest.

■ ACKNOWLEDGMENTS

We are grateful for generous financial support from the National Science Foundation (DMR-0856009 and DMR-0906727), the Robert A. Welch Foundation (E-1320), and the Texas Center for Superconductivity at the University of Houston.

■ REFERENCES

(1) Love, J. C.; Estroff, L. A.; Kriebel, J. K.; Nuzzo, R. G.; Whitesides, G. M. Self-Assembled Monolayers of Thiolates on Metals as a Form of Nanotechnology. *Chem. Rev.* **2005**, *105*, 1103−1170.

(2) Ulman, A. Formation and Structure of Self-Assembled Monolayers. *Chem. Rev.* **1996**, *96*, 1533−1554.

(3) Bain, C. D.; Troughton, E. B.; Tao, Y. T.; Evall, J.; Whitesides, G. M.; Nuzzo, R. G. Formation of Monolayer Films by the Spontaneous Assembly of Organic Thiols from Solution onto Gold. *J. Am. Chem. Soc.* **1989**, *111*, 321−335.

(4) Hosseinpour, S.; Johnson, C. M.; Leygraf, C. Alkanethiols as Inhibitors for the Atmospheric Corrosion of Copper Induced by Formic Acid: Effect of Chain Length. *J. Electrochem. Soc.* **2013**, *160*, C270−C276.

(5) Laibinis, P. E.; Whitesides, G. M. Self-Assembled Monolayers of N-Alkanethiolates on Copper Are Barrier Films That Protect the Metal against Oxidation by Air. *J. Am. Chem. Soc.* **1992**, *114*, 9022−9028.

(6) Jennings, G. K.; Laibinis, P. E. Self-Assembled Monolayers of Alkanethiols on Copper Provide Corrosion Resistance in Aqueous Environments. *Colloids Surf., A* **1996**, *116*, 105−114.

(7) Petrović, Ž.; Metikoš-Huković, M.; Babić, R. Modification of Copper with Self-Assembled Organic Coatings. *Prog. Org. Coat.* **2008**, *61*, 1−6.

(8) Hutt, D. A.; Liu, C. Oxidation Protection of Copper Surfaces Using Self-Assembled Monolayers of Octadecanethiol. *Appl. Surf. Sci.* **2005**, *252*, 400−411.

(9) Zamborini, F. P.; Crooks, R. M. Corrosion Passivation of Gold by N-Alkanethiol Self-Assembled Monolayers: Effect of Chain Length and End Group. *Langmuir* **1998**, *14*, 3279−3286.

(10) Deng, K.; Collins, R. J.; Mehregany, M.; Sukenik, C. N. Performance Impact of Monolayer Coating of Polysilicon Micromotors. *J. Electrochem. Soc.* **1995**, *142*, 1278−1285.

(11) Shao, J.; Josephs, E. A.; Lee, C.; Lopez, A.; Ye, T. Electrochemical Etching of Gold within Nanoshaved Self-Assembled Monolayers. *ACS Nano* **2013**, *7*, 5421.

(12) Widrig, C. A.; Chung, C.; Porter, M. D. The Electrochemical Desorption of N-Alkanethiol Monolayers from Polycrystalline Au and Ag Electrodes. *J. Electroanal. Chem.* **1991**, *310*, 335−359.

(13) Yang, D. F.; Wilde, C. P.; Morin, M. Studies of the Electrochemical Removal and Efficient Re-Formation of a Monolayer of Hexadecanethiol Self-Assembled at an Au(111) Single Crystal in Aqueous Solutions. *Langmuir* **1997**, *13*, 243−249.

(14) Byloos, M.; Al-Maznai, H.; Morin, M. Phase Transitions of Alkanethiol Self-Assembled Monolayers at an Electrified Gold Surface. *J. Phys. Chem. B* **2001**, *105*, 5900−5905.

(15) Kim, M.; Hohman, J. N.; Morin, E. I.; Daniel, T. A.; Weiss, P. S. Self-Assembled Monolayers of 2-Adamantanethiol on Au{111}: Control of Structure and Displacement. *J. Phys. Chem. A* **2009**, *113*, 3895−3903.

(16) Badia, A.; Cuccia, L.; Demers, L.; Morin, F.; Lennox, R. B. Structure and Dynamics in Alkanethiolate Monolayers Self-Assembled on Gold Nanoparticles: A DSC, FT-IR, and Deuterium NMR Study. *J. Am. Chem. Soc.* **1997**, *119*, 2682−2692.

(17) Ghaly, T.; Wildt, B. E.; Searson, P. C. Electrochemical Release of Fluorescently Labeled Thiols from Patterned Gold Surfaces. *Langmuir* **2009**, *26*, 1420−1423.

(18) Hamoudi, H.; Chesneau, F.; Patze, C.; Zharnikov, M. Chain-Length-Dependent Branching of Irradiation-Induced Processes in

Alkanethiolate Self-Assembled Monolayers. *J. Phys. Chem. C* **2010**, *115*, 534−541.
(19) Jiang, X.; Ferrigno, R.; Mrksich, M.; Whitesides, G. M. Electrochemical Desorption of Self-Assembled Monolayers Noninvasively Releases Patterned Cells from Geometrical Confinements. *J. Am. Chem. Soc.* **2003**, *125*, 2366−2367.
(20) Walczak, M. M.; Alves, C. A.; Lamp, B. D.; Porter, M. D. Electrochemical and X-ray Photoelectron Spectroscopic Evidence for Differences in the Binding Sites of Alkanethiolate Monolayers Chemisorbed at Gold. *J. Electroanal. Chem.* **1995**, *396*, 103−114.
(21) Sun, K.; Jiang, B.; Jiang, X. Electrochemical Desorption of Self-Assembled Monolayers and Its Applications in Surface Chemistry and Cell Biology. *J. Electroanal. Chem.* **2011**, *656*, 223−230.
(22) Abbott, N. L.; Gorman, C. B.; Whitesides, G. M. Active Control of Wetting Using Applied Electrical Potentials and Self- Assembled Monolayers. *Langmuir* **1995**, *11*, 16−18.
(23) Wilhelm, T.; Wittstock, G. Patterns of Functional Proteins Formed by Local Electrochemical Desorption of Self-Assembled Monolayers. *Electrochim. Acta* **2001**, *47*, 275−281.
(24) Mali, P.; Bhattacharjee, N.; Searson, P. C. Electrochemically Programmed Release of Biomolecules and Nanoparticles. *Nano Lett.* **2006**, *6*, 1250−1253.
(25) Choi, S.; Chae, J. A Regenerative Biosensing Surface in Microfluidics Using Electrochemical Desorption of Short-Chain Self-Assembled Monolayer. *Microfluid. Nanofluid.* **2009**, *7*, 819−827.
(26) Loglio, F.; Schweizer, M.; Kolb, D. M. In Situ Characterization of Self-Assembled Butanethiol Monolayers on Au(100) Electrodes. *Langmuir* **2002**, *19*, 830−834.
(27) Byloos, M.; Al-Maznai, H.; Morin, M. Formation of a Self-Assembled Monolayer Via the Electrospreading of Physisorbed Micelles of Thiolates. *J. Phys. Chem. B* **1999**, *103*, 6554−6561.
(28) Kondo, T.; Sumi, T.; Uosaki, K. A Rotating Gold Ring−Gold Disk Electrode Study on Electrochemical Reductive Desorption and Oxidative Readsorption of a Self-Assembled Monolayer of Dodecanethiol. *J. Electroanal. Chem.* **2002**, *538*−*539*, 59−63.
(29) Pesika, N. S.; Stebe, K. J.; Searson, P. C. Kinetics of Desorption of Alkanethiolates on Gold. *Langmuir* **2006**, *22*, 3474−3476.
(30) Yang, D. F.; Al-Maznai, H.; Morin, M. Vibrational Study of the Fast Reductive and the Slow Oxidative Desorptions of a Nonanethiol Self-Assembled Monolayer from a Au(111) Single Crystal Electrode. *J. Phys. Chem. B* **1997**, *101*, 1158−1166.
(31) Cai, X.; Baldelli, S. Surface Barrier Properties of Self-Assembled Monolayers as Deduced by Sum Frequency Generation Spectroscopy and Electrochemistry. *J. Phys. Chem. C* **2011**, *115*, 19178−19189.
(32) Nečas, D.; Klapetek, P. Gwyddion: An Open-Source Software for Spm Data Analysis. *Cent. Eur. J. Phys.* **2012**, *10*, 181−188.
(33) Cimatu, K.; Baldelli, S. Chemical Imaging of Corrosion: Sum Frequency Generation Imaging Microscopy of Cyanide on Gold at the Solid−Liquid Interface. *J. Am. Chem. Soc.* **2008**, *130*, 8030−8037.
(34) Jacob, J. D. C.; Rittikulsittichai, S.; Lee, T. R.; Baldelli, S. Characterization of Sams Derived from Octadecyloxyphenylethanethiols by Sum Frequency Generation. *J. Phys. Chem. C* **2013**, *117*, 9355−9365.
(35) Himmelhaus, M.; Eisert, F.; Buck, M.; Grunze, M. Self-Assembly Ofn-Alkanethiol Monolayers. A Study by Ir−Visible Sum Frequency Spectroscopy (Sfg). *J. Phys. Chem. B* **2000**, *104*, 576−584.
(36) Yee, S.; Chang, O.-K. A Simple Junction for Reference Electrodes. *J. Chem. Educ.* **1988**, *65*, 129.
(37) Ong, T. H.; Davies, P. B.; Bain, C. D. Sum-Frequency Spectroscopy of Monolayers of Alkoxy-Terminated Alkanethiols in Contact with Liquids. *Langmuir* **1993**, *9*, 1836−1845.
(38) Hirose, C.; Yamamoto, H.; Akamatsu, N.; Domen, K. Orientation Analysis by Simulation of Vibrational Sum Frequency Generation Spectrum: CH Stretching Bands of the Methyl Group. *J. Phys. Chem.* **1993**, *97*, 10064−10069.
(39) Hirose, C.; Akamatsu, N.; Domen, K. Formulas for the Analysis of Surface Sum-Frequency Generation Spectrum by CH Stretching Modes of Methyl and Methylene Groups. *J. Chem. Phys.* **1992**, *96*, 997−1004.
(40) Wang, H. F.; Gan, W.; Lu, R.; Rao, Y.; Wu, B. H. Quantitative Spectral and Orientational Analysis in Surface Sum Frequency Generation Vibrational Spectroscopy (Sfg-Vs). *Int. Rev. Phys. Chem.* **2005**, *24*, 191−256.
(41) Alexiadis, O.; Harmandaris, V. A.; Mavrantzas, V. G.; Site, L. D. Atomistic Simulation of Alkanethiol Self-Assembled Monolayers on Different Metal Surfaces Via a Quantum, First-Principles Parametrization of the Sulfur−Metal Interaction. *J. Phys. Chem. C* **2007**, *111*, 6380−6391.
(42) Doneux, T.; Nichols, R. J.; Buess-Herman, C. Dissolution Kinetics of Octadecanethiolate Monolayers Electro-Adsorbed on Au(111). *J. Electroanal. Chem.* **2008**, *621*, 267−276.
(43) Chai, L.; Klein, J. Large Area, Molecularly Smooth (0.2 Nm Rms) Gold Films for Surface Forces and Other Studies. *Langmuir* **2007**, *23*, 7777−7783.
(44) Sondag-Huethorst, J. A. M.; Fokkink, L. G. J. Potential-Dependent Wetting of Octadecanethiol-Modified Polycrystalline Gold Electrodes. *Langmuir* **1992**, *8*, 2560−2566.
(45) Lee, L. Y.; Lennox, R. B. Electrochemical Desorption of N-Alkylthiol Sams on Polycrystalline Gold: Studies Using a Ferrocenylalkylthiol Probe. *Langmuir* **2007**, *23*, 292−296.
(46) Yang, D. F.; Wilde, C. P.; Morin, M. Electrochemical Desorption and Adsorption of Nonyl Mercaptan at Gold Single Crystal Electrode Surfaces. *Langmuir* **1996**, *12*, 6570−6577.
(47) Doneux, T.; Steichen, M.; De Rache, A.; Buess-Herman, C. Influence of the Crystallographic Orientation on the Reductive Desorption of Self-Assembled Monolayers on Gold Electrodes. *J. Electroanal. Chem.* **2010**, *649*, 164−170.
(48) Wong, S. S.; Porter, M. D. Origin of the Multiple Voltammetric Desorption Waves of Long-Chain Alkanethiolate Monolayers Chemisorbed on Annealed Gold Electrodes. *J. Electroanal. Chem.* **2000**, *485*, 135−143.
(49) Kawaguchi, T.; Yasuda, H.; Shimazu, K.; Porter, M. D. Electrochemical Quartz Crystal Microbalance Investigation of the Reductive Desorption of Self-Assembled Monolayers of Alkanethiols and Mercaptoalkanoic Acids on Au. *Langmuir* **2000**, *16*, 9830−9840.
(50) C, N., III; Chidsey, C. E. D.; Liu, G.-y.; Scoles, G. Substrate Dependence of the Surface Structure and Chain Packing of Docosyl Mercaptan Self-Assembled on the (111), (110), and (100) Faces of Single Crystal Gold. *J. Chem. Phys.* **1993**, *98*, 4234−4245.
(51) Weisshaar, D. E.; Walczak, M. M.; Porter, M. D. Electrochemically Induced Transformations of Monolayers Formed by Self-Assembly of Mercaptoethanol at Gold. *Langmuir* **1993**, *9*, 323−329.
(52) Schneider, T. W.; Buttry, D. A. Electrochemical Quartz Crystal Microbalance Studies of Adsorption and Desorption of Self-Assembled Monolayers of Alkyl Thiols on Gold. *J. Am. Chem. Soc.* **1993**, *115*, 12391−12397.
(53) Mulder, W. H.; Calvente, J. J.; Andreu, R. A Kinetic Model for the Reductive Desorption of Self-Assembled Thiol Monolayers. *Langmuir* **2001**, *17*, 3273−3280.
(54) Poelman, M.; Buess-Herman, C.; Badiali, J. P. Kinetics of Disordering of Two-Dimensional Organic Phases at the Electrochemical Interface. *Langmuir* **1999**, *15*, 2194−2201.
(55) Wang, W.; Zhang, S. S.; Chinwangso, P.; Advincula, R. C.; Lee, T. R. Electric Potential Stability and Ionic Permeability of Sams on Gold Derived from Bidentate and Tridentate Chelating Alkanethiols. *J. Phys. Chem. C* **2009**, *113*, 3717−3725.
(56) Boubour, E.; Lennox, R. B. Potential-Induced Defects in N-Alkanethiol Self-Assembled Monolayers Monitored by Impedance Spectroscopy. *J. Phys. Chem. B* **2000**, *104*, 9004−9010.
(57) Boubour, E.; Lennox, R. B. Insulating Properties of Self-Assembled Monolayers Monitored by Impedance Spectroscopy. *Langmuir* **2000**, *16*, 4222−4228.
(58) Boubour, E.; Lennox, R. B. Stability of Ω-Functionalized Self-Assembled Monolayers as a Function of Applied Potential. *Langmuir* **2000**, *16*, 7464−7470.
(59) Sahalov, H.; O'Brien, B.; Stebe, K. J.; Hristova, K.; Searson, P. C. Influence of Applied Potential on the Impedance of Alkanethiol Sams. *Langmuir* **2007**, *23*, 9681−9685.

(60) Schlenoff, J. B.; Li, M.; Ly, H. Stability and Self-Exchange in Alkanethiol Monolayers. *J. Am. Chem. Soc.* **1995**, *117*, 12528−12536.
(61) Casanova-Moreno, J. R.; Bizzotto, D. What Happens to the Thiolates Created by Reductively Desorbing Sams? An in Situ Study Using Fluorescence Microscopy and Electrochemistry. *Langmuir* **2013**, *29*, 2065−2074.